

Tribology challenges of modern magnetic hard disk drives

Andrei Khurshudov*, Robert J. Waltman

IBM, Storage Technology Division, San Jose, CA 95193, USA

Abstract

This paper reviews the effect of the design evolution of modern magnetic hard disk drives on tribological challenges, such as wearless high-speed contact, ultra-thin lubrication, corrosion protection, and requirements of thinner carbon overcoat. We will present some data on slider wear measurements on the order of nanometers, lubricant migration and depletion as linked to tribological reliability, lubricant bonding kinetics on different carbon overcoats, corrosion protection using lubricant and thin carbon coatings, and lubricant de-wetting. © 2001 Elsevier Science B.V. All rights reserved.

Keywords: Hard disk drive; Durability; Lubricant properties; Future trends

1. Introduction

Modern hard disk drive represents a unique combination of the latest technologies in tribology, thin film deposition, fluid mechanics, magnetism, and material science. While trying to achieve the market leadership, disk drive manufacturers are continually pushing design requirements beyond previous limits. A real density is growing at about 100% per year. Mechanical spacing between the slider and the disk is steadily reduced. The disk rpm is heading towards 20,000 and beyond. Under these circumstances, drive performance improvement has to be necessarily combined with high mechanical and tribological durability to maintain user satisfaction.

In this work, we address some of the tribological challenges of the modern head–disk interface associated with lower flying heights and a reduction in the thickness of the protective carbon and lubricant layers. An understanding of these interfacial phenomena will provide the direction for resolution of these challenges.

2. Results and discussion

2.1. Wear at the contact interface and its measurement

When a fast-flying slider is brought into contact with the disk surface, mechanical wear will inevitably take place on both the disk and slider surfaces. This wear is small in scale — on the order of nanometers — thus, difficult to

detect or quantify. For the wear measurement on sliders, two main techniques are employed:

- Raman spectroscopy, where the intensity of the G and D peaks in the spectrum is calibrated against the thickness change in the carbon [1].
- Surface marking by nanoindentation or focused ion beam (FIB) methodologies [2,3]. The dimensions of the marked area change as a function of surface wear and so may be quantified.

Both techniques measure the wear rate of the slider due to contact.

The results of a wear measurement on the slider provides significant insight. Fig. 1 shows that the wear rate of a contact recording slider, measured at the trailing edge of a slider during a 7-day test, is quite significant. The wear rate was measured by recording the changes in the height of the contact pad at the trailing edge of the slider, using atomic force microscopy (AFM). The slider was flying nominally at 2 nm (as measured using a dynamic flying height Tester), at a velocity of 8 m/s, with approximately 4–5 nm interference with the disk surface. Fig. 1 shows that the 40 Å carbon film on the slider is worn away within 2 days with the wear rate decreasing significantly thereafter. The figure also shows that after 2 days, the contact surface of the slider no longer has the protective carbon film, allowing exposure of the disk lubricant to bare alumina. In today's disk drives, perfluoropolyethers are widely used as the topical lubricant. Studies on the interaction of perfluoropolyether lubricants and catalytic surfaces such as alumina indicate that chemical degradation of the perfluoropolyether lubricant can occur [4–11]. In addition, the debris generated by the carbon wear may contribute to the particulate contamination of the interface.

* Corresponding author. Tel.: +1-408-578-1652; fax: +1-408-256-2410.
E-mail address: andreik@us.ibm.com (A. Khurshudov).

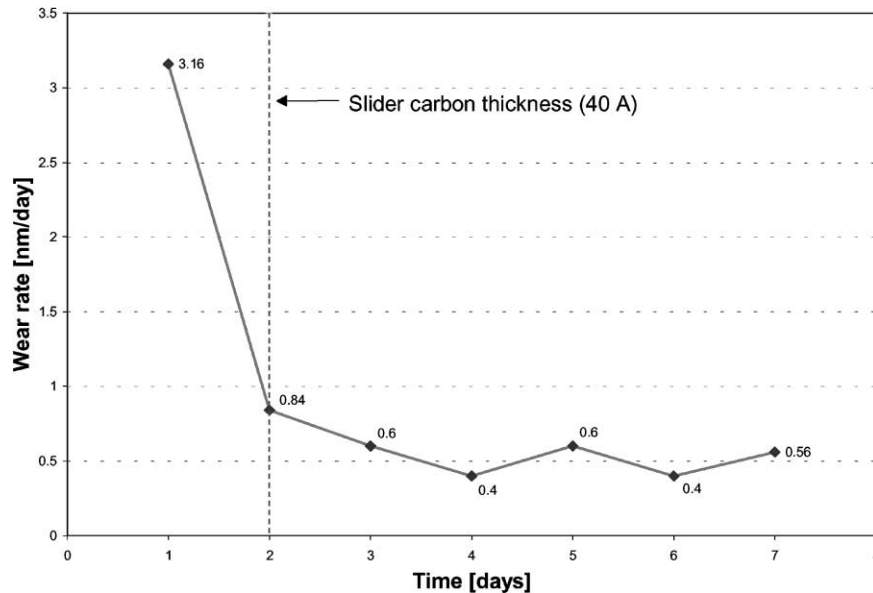


Fig. 1. Wear at the trailing edge of a sub-ambient pressure slider. The flying height (FH) is equal to ~ 2 nm at a velocity of 8 m/s. The flying height was measured using a dynamic flying height tester.

Wear of the disk surface is much more difficult to quantify using traditional techniques (i.e. [12]); however, recent work indicates that the application of the optical surface analyzer (OSA) [13] can be particularly revealing. The OSA methodology is based upon the measurement of the reflected portion of polarized light from the disk surface at the Brewster's angle. The interpretation of the images has been discussed previously [13]. Fig. 2 shows a 3 mm wide section of the disk in S and P polarized light. As shown in the figure, the wear in the carbon is readily observed. With suitable calibration between carbon thickness and reflectivity changes, the wear is readily quantified. The wear depth in the carbon in Fig. 2 is estimated to be around 2.5 \AA .

In fact, the same optical technique can be applied to wear measurements on the slider after an appropriate calibration procedure.

The process of initial interfacial wearing (or burnishing) of the finished disk surface is beneficial because it min-

imizes interference and vibrations between the slider and disk. Unfortunately, burnishing also generates wear particles that can significantly affect the magnetic performance of the head by exciting vibrations of the suspension. Also, a particle trapped at the interface may lead to an early failure of the protective overcoat(s).

2.2. Wear particles at the contact interface

The results in the previous section demonstrate that even the cleanest manufacturing and assembly process cannot prevent particles from collecting at the slider-disk interface, as they are almost always generated during the slider-disk contact. Particles are especially harmful when low-flying sliders are used and the slider-disk clearance is close to zero. Therefore, knowledge of particle generation, occurrence, migration, trapping and interactions at the head-disk interface (HDI) may provide

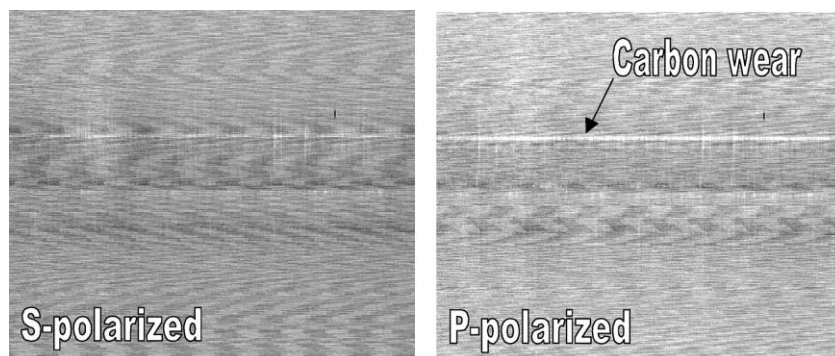


Fig. 2. Disk wear after 72 h of testing for low-flying positive pressure slider. FH ~ 5 nm at 8 m/s.

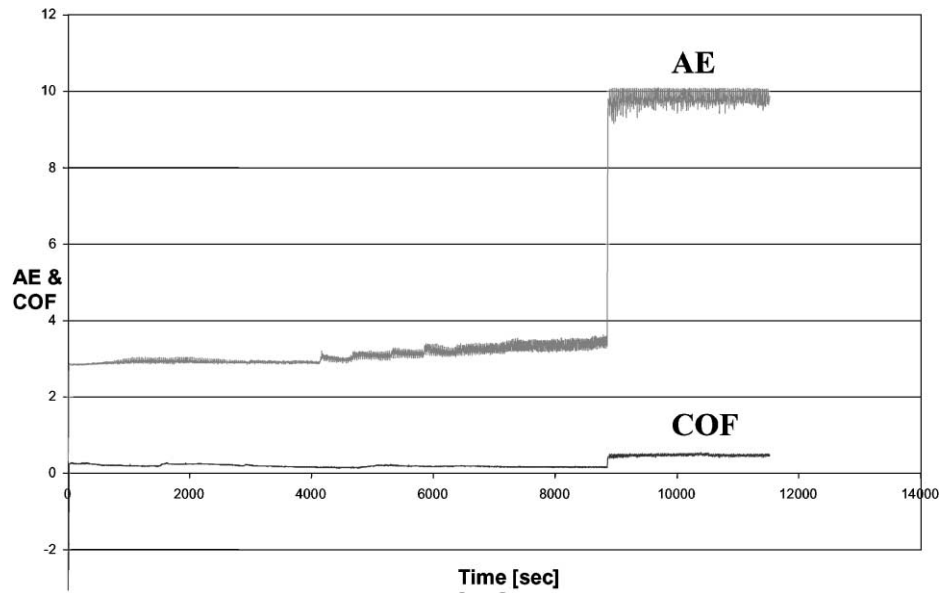


Fig. 3. Transition in the AE and friction due to the particle(s) trapped at the interface.

direction for the design of a more particle-tolerant interface.

Fig. 3 shows just how quickly a change in slider–disk interaction occurs when a particle is trapped at the HDI; instantly, the coefficient of friction (COF) is observed to increase from almost 0 (flying head) to 0.25. Concomitantly, the acoustic emission (AE) signal increases, in this instance by $\sim 3\times$, indicative of slider–body vibrations.

Fig. 4 below illustrates the results of an experiment designed to investigate particle migration in the HDI. The same sub-ambient pressure slider is flown over several different disks prepared identically, i.e. same carbon and lubricant thickness and composition. The disks are designated in the

figure as 003A, 003B, 004A, etc. Each unique three-digit number represents a sister disk with the A or B designation following the three-digit mnemonic defining the A- or B-side, respectively. Flying with the same slider, both 003 and 004 disks show little interference between slider and disk (0–400 s). However, a sharp transition in both AE and COF is observed upon the introduction of disk 008 (400–600 s). Subsequently, disk 008 is replaced with the previously measured disk 003, however, now produces high AE and COF signals with the same slider (600–800 s). At 800 s, the same slider was cleaned and then the disk 003 was re-tested with the cleaned slider. With the cleaned slider, the AE and COF returns to nominal values (800–900 s) recorded

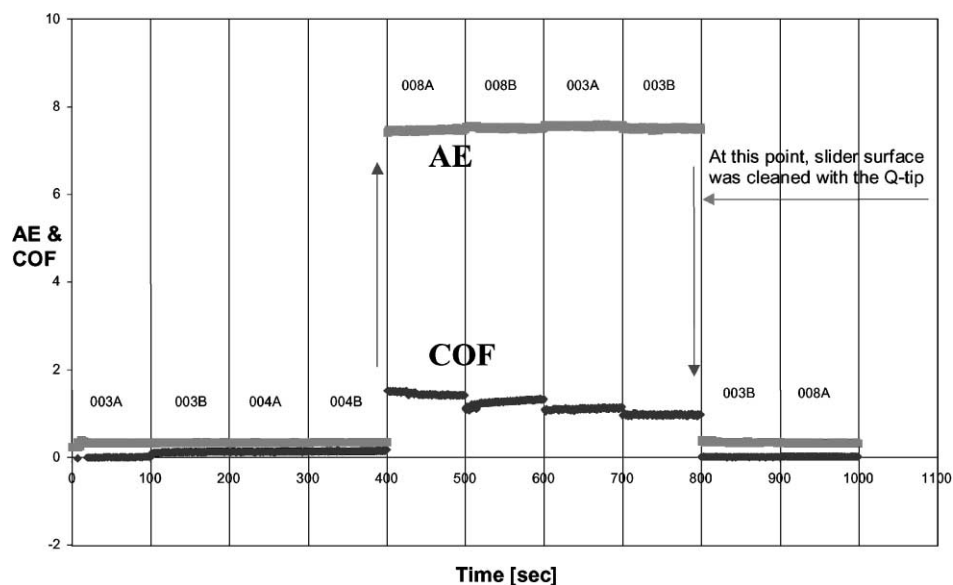


Fig. 4. Evolution of the AE and coefficient of friction from one disk to another.

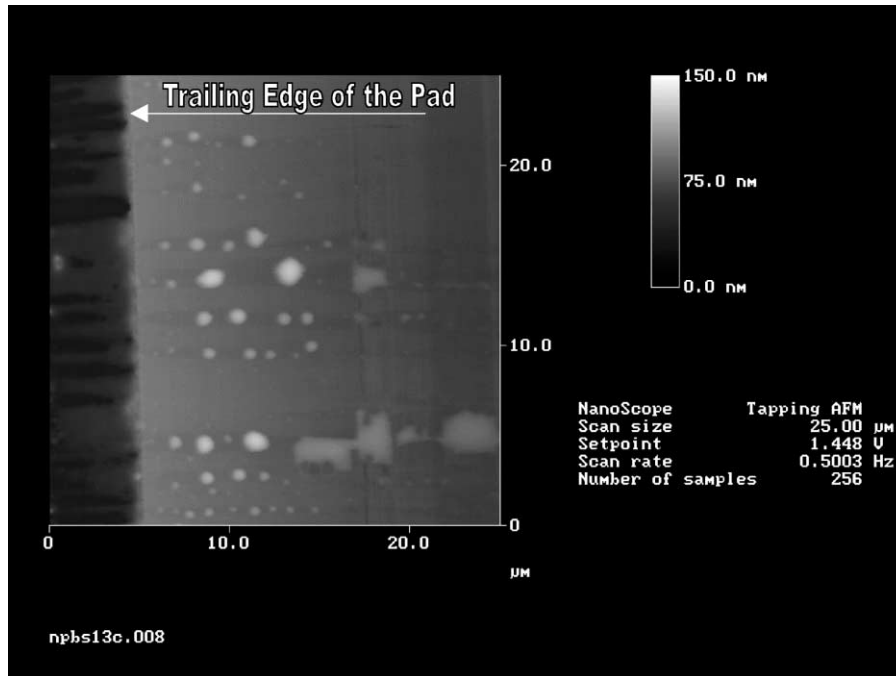


Fig. 5. AFM image of the trailing edge pad of a sub-ambient pressure slider in the middle of slider–disk burnishing.

initially. Finally, disk 008 was re-tested (900–1000 s) only to show nominal AE and COF signals. These data indicate particle transfer to the slider, generated during slider–disk contacts, as the primary reason for the observed interference.

We interpret these data as an indication that the “wear particles” become wedged between the slider and the disk, causing a plowing of the disk surface with the observed increase in contact force and both AE and friction. An otherwise gradual increase in AE with time prior to a sharp increase implies (see Fig. 3) wear particle accumulation until a critical level is attained. The slider’s negative pressure promotes particle accumulation on the slider surface, where they are possibly mixed with the lubricant. Fig. 5 shows the AFM image of the slider’s trailing edge pad with the droplet accumulation. They are lubricant, possibly mixed with wear particles.

On the basis of these experiments, we may conclude that particulate contaminants are readily transferred to the slider surface even if they originate on the disk surface. When they are trapped in the gap between the slider and the disk, their presence can be inferred by the increased AE and COF signals. This results in slider vibrations and magnetic errors, which are significant limiting factors in the implementation of contact magnetic recording today.

2.3. Lubricant mobility and its effect on tribological durability

Before any real wear of the carbon film takes place, the overlying lubricant film is expected to be first displaced from the contact interface. A typical perfluoropolyether lubricant

layer in today’s hard disk drives is $<20 \text{ \AA}$ thick, and consists of both bonded and mobile fractions.

When the slider interacts with the disk surface, the expectation is that it first mechanically displaces the mobile lubricant after which, it acts upon any bonded lubricant. Fig. 6 shows an entire interface failure cycle, as recorded by the OSA, using a low speed sliding test whereby the slider is dragged in contact over the disk surface.

Depletion of the mobile lubricant occurs initially at the places of contact by lubricant displacement to the outside of the contact track. This displacement causes the lubricant to accumulate or “pool” in regions adjacent to the track causing lubricant thickness changes and non-uniformity [13]. With continued “dragging” in the same wear track, the bonded lubricant is also eventually displaced. Catastrophic failure occurs when carbon wear ensues. Since the mobile lubricant in the pooled region can flow, it can migrate back onto the wear track to prevent damage. If the rate of re-flow is higher than the rate of depletion from the contacted track, frictional wear is mitigated [14]. Thus, optimization of interface durability requires a balance between lubricant properties such as thickness and mobility, and lubricant stability (e.g. bonding). The effect of lubricant mobility on drag durability is illustrated in Fig. 7.

Under the conditions of the test, 15 \AA of fully bonded Zdol 4000 on a CN_x disk fails after $\sim 37,000$ drag cycles. When 5 \AA of mobile Zdol 4000 is additionally coated onto the disk, the drag durability increases by a factor of $\sim 8\times$. Therefore, it is tribologically beneficial to have mobile lubricant on the disk surface. The mobility of the lubricant on the disk surface is dependent upon the internal parameters

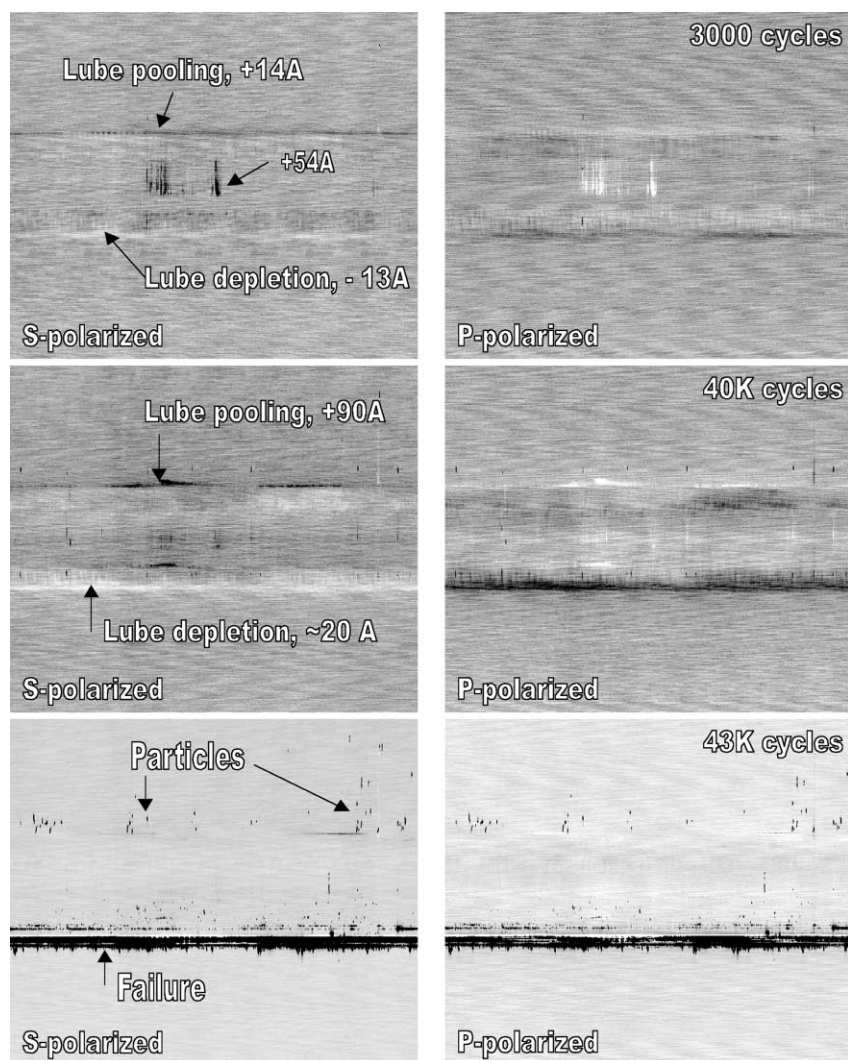


Fig. 6. Changes in the disk surface with increasing drag cycles as observed by in situ OSA. The initial lubricant (Zdol) thickness is 20 Å.

of the lubricant such as chain flexibility; lubricant–surface interactions; and external parameters such as temperature. In the next section, we briefly demonstrate the effect of some of these parameters.

2.4. Lubricant bonding kinetics and mobility on different carbon overcoats

Bonding kinetics profiles for 11 Å films of Zdol 4000 as a function of lubricant and carbon parameters are presented in Fig. 8. These data reveal that the bonding of Zdol on carbon is a time-dependent phenomenon [15]. The focal point of these studies is an investigation of how changes in lubricant and/or carbon structure influence the bonding kinetics. To clarify the effect of lubricant structure, we note that the Zdol class of lubricants is a random copolymer of perfluoromethylene oxide and perfluoroethylene oxide units, capped by hydroxyl end groups. In the ensuing discussion, we design-

nate the CF_2O monomer unit as “C1” and the $\text{CF}_2\text{CF}_2\text{O}$ monomer unit as “C2”.

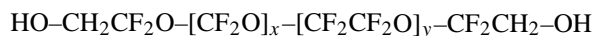


Fig. 8 (top, left) illustrates the dramatically different bonding kinetics that are observed simply by varying the C1 and C2 ratio in Zdol. The CH_x carbon films employed in this study are identical. For Zdol 4000 with the higher C1:C2 ratio of 1.34, the bonding rate coefficient $k \propto 1/t$, while at the relatively lower C1:C2 ratio of 0.89, $k \propto 1/\sqrt{t}$. When $k \propto 1/t$, the bonding kinetics profile is initially rapid characterized by a concave downwards curve. In contrast, when $k \propto 1/\sqrt{t}$, the initial bonding rate is comparatively smaller characterized by an initially concave upwards curve. As shown in the figure, the bonded fraction that is ultimately attained is significantly larger for bonding kinetics that follow $k \propto 1/\sqrt{t}$ kinetics. From a tribological view, e.g. Fig. 7, significant bonding could result in a less durable interface. The origin

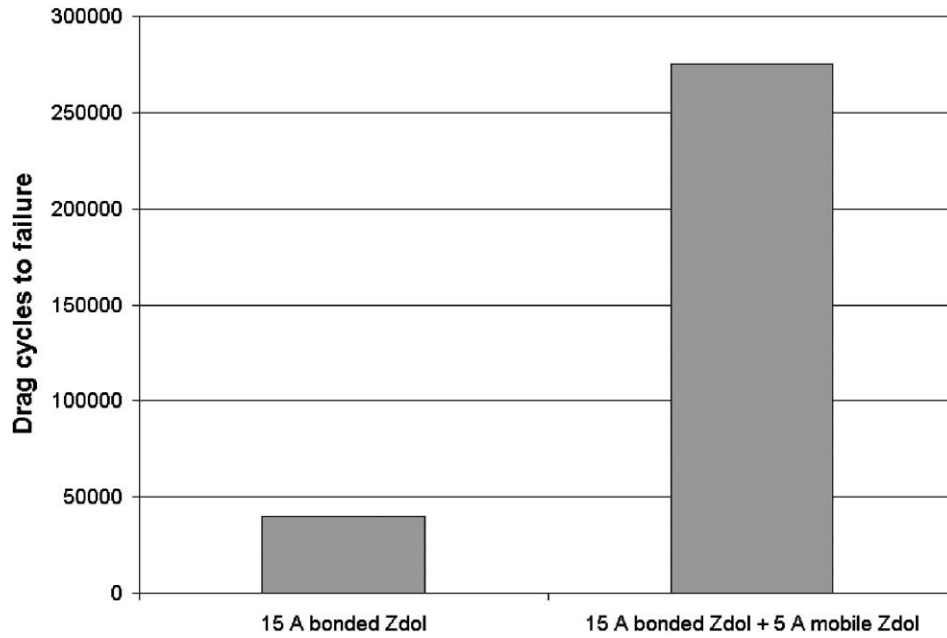


Fig. 7. The effect of Zdol 4000 mobility on low speed (0.6 m/s) drag durability.

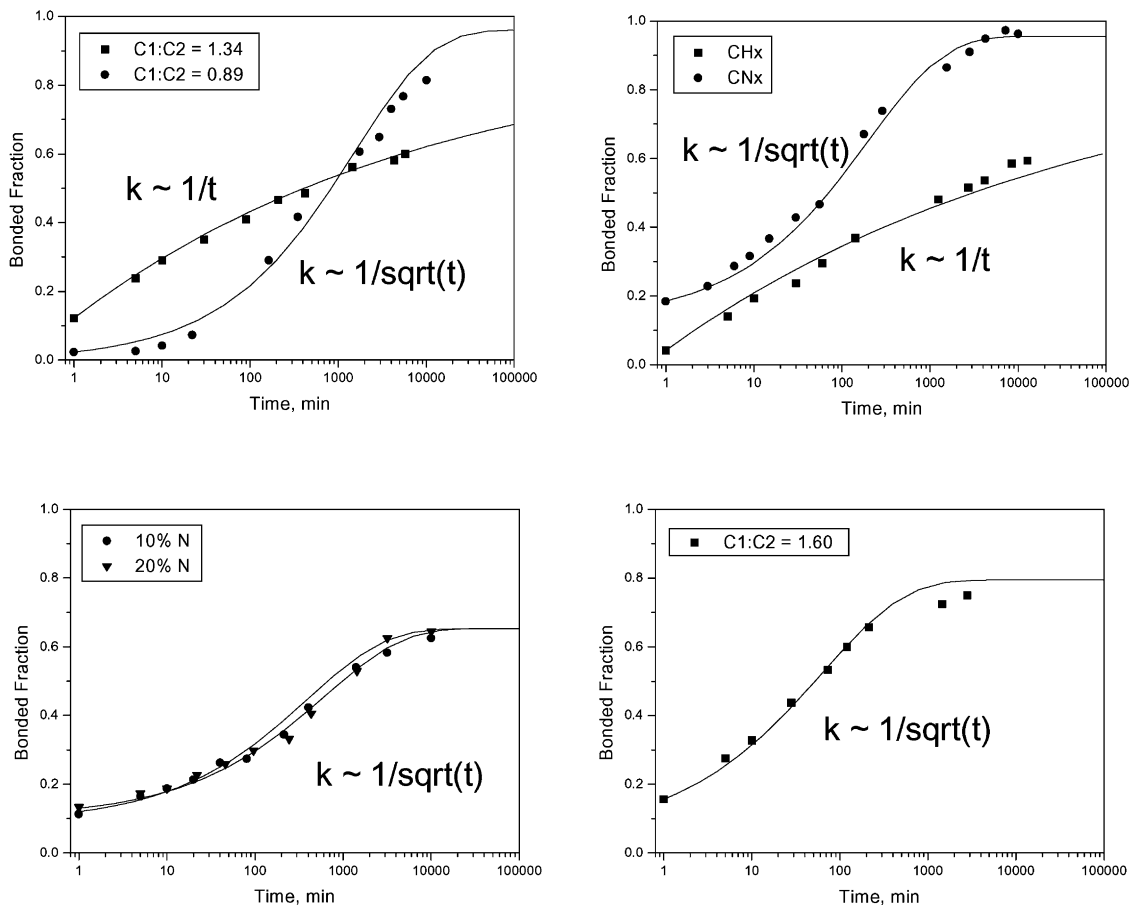


Fig. 8. Evolution of bonded lubricant as a function of annealing time: (top, left) Zdol 4000 as a function of time and the C1:C2 ratio on CH_x at 64°C and 4% RH; (top, right) Zdol 4000 (C1:C2 = 1.09) on CH_x vs. CN_x at 64°C and 4% RH; (bottom, left) Zdol 2000 (C1:C2 = 1.12) on CN_x (% N) at 64°C and 4% RH; and (bottom, right) Zdol 4000 (C1:C2 = 1.60) on CN_x at 90°C and <2% RH.

Table 1

Titrated Zdol thickness (maximum bonded thickness) (Å) on (AlMg)-CH_x and CN_x

Zdol molecular weight	CH _x	CN _x (10% nitrogen)	CN _x (20% nitrogen)
1100	6	8	8
2000	14	22	22
4000	25	39	39

for the different bonding kinetics is explained on the basis of bonding that occurs from a more liquid-like ($k \propto 1/t$) or more solid-like ($k \propto 1/\sqrt{t}$) Zdol [16]. The differences have been interpreted on the basis of barriers to internal rotation about C1 and C2 structural moieties [17].

In Fig. 8 (top, right), the bonding kinetics of identical Zdol 4000 (C1:C2 = 1.09) on CH_x and CN_x (10% N atomic composition) are compared. Zdol 4000 with the relatively higher C1:C2 ratio of 1.09 produces the expected $k \propto 1/t$ bonding kinetics on CH_x. In contrast, the same Zdol on CN_x exhibits instead the $k \propto 1/\sqrt{t}$, previously attributed to stiffer Zdol chains. Even when an extremely flexible Zdol chain is employed on CN_x (10% N atomic composition), Fig. 8 (bottom, right), where the Zdol C1:C2 = 1.60, the bonding profile kinetics can still be described by the $k \propto 1/\sqrt{t}$ dependence. The origin for this difference is explained on the basis of the more repulsive intermolecular interactions between Zdol and CN_x [18,19], and the resultant differences in their adsorbed film structure. Lubricant titration studies as a function of Zdol molecular weight, Table 1, indicate that more Zdol can be packed into a monolayer on CN_x than on CH_x. Thus, CN_x imposes greater confinement of the Zdol adsorbed layer compared to the CH_x surface.

In Fig. 8 (bottom, left), the bonding kinetics of identical Zdol 2000 (C1:C2 = 1.12) on CN_x, as a function of % nitrogen, are compared. At both 10 and 20% nitrogen, the $k \propto 1/\sqrt{t}$ bonding kinetics is preserved and the bonding rates are very similar. Table 1 reveals that the titrated thickness for Zdols for CN_x with 10 and 20% nitrogen are identical, hence, the Zdols interact with both CN_x films in a similar way. Thus, these studies reveal that the bonding kinetics are most influenced by lubricant chain stiffness, and adsorbed film structure.

2.5. Disk corrosion protection and the role of lubricant

Another challenge facing tribological reliability stems from the continuously decreasing thickness of the carbon overcoat film. Fig. 9 shows the effect of carbon overcoat thickness on the number of corrosion spots on both CH_x and CN_x. When the carbon film thickness is greater than ~ 80 Å, the number of corrosion spots asymptotes to an intrinsic level characteristic of the carbon film (i.e. surface oxide concentration, porosity, etc.).

When the carbon film thickness decreases below ~ 50 Å, the number of corrosion spots begins to increase gradually. However, for carbon film thickness less than ~ 25 Å, the corrosion level increases by an order of magnitude as the carbon film becomes compromised. This is indicative of an inability of the thin carbon film, at least as sputtered in a typical manufacturing process, to protect the magnetic media from corrosion, in addition to raising questions regarding its tribological reliability and scratch resistance. Corrosion occurs at the head-disk interface as small corrosion spots, typically, a few microns in diameter,

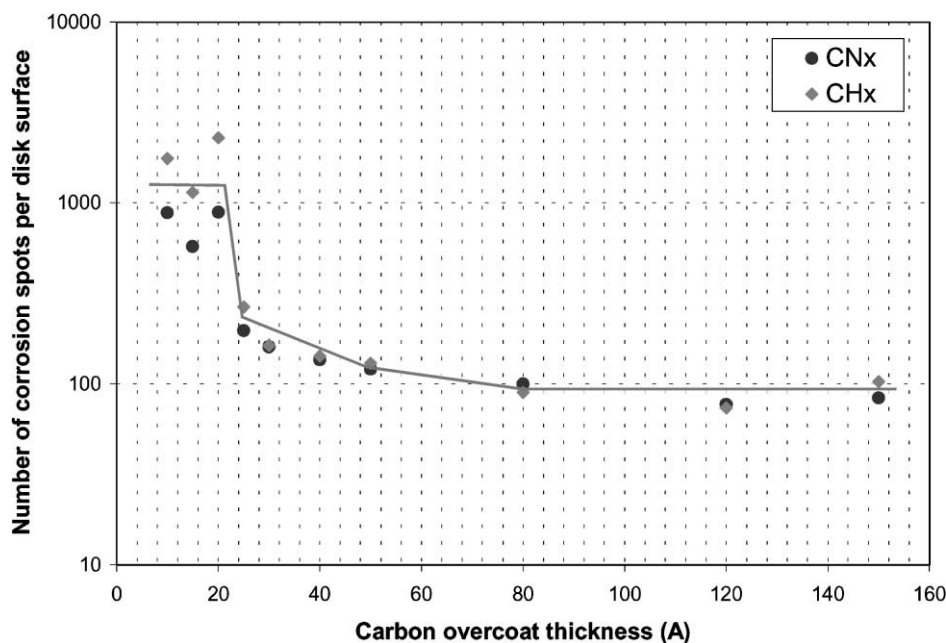


Fig. 9. The number of corrosion spots as a function of carbon thickness after exposure to 80°C and 90% RH for 7 days. All disks had a constant Zdol 4000 thickness of 14 Å.

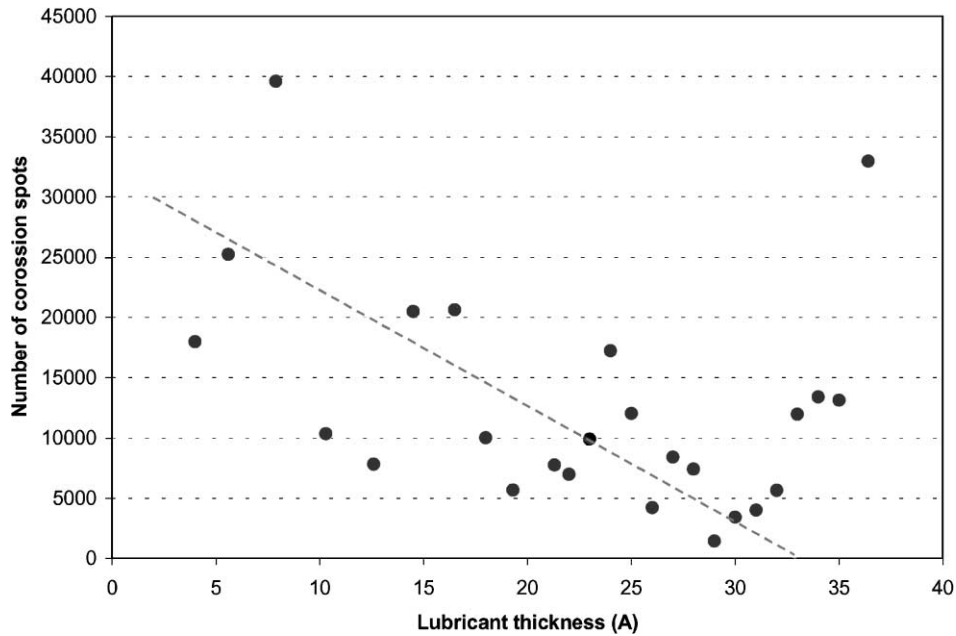


Fig. 10. The number of corrosion spots on a disk as a function of Zdol 4000 thickness on (glass) CN_x as measured by OSA.

and a few dozens of nanometer high. The corrosion spots can interfere with the flying slider and affect tribological reliability.

There are more than several ways by which disk corrosion may be mitigated. A lubricant approach would be to either increase the bonded fraction or increase the film thickness. Selection of the appropriate bonded fraction and/or lubricant film thickness would ultimately be tempered by tribological impact. However, it can be expected that corrosion of the disk surface will decrease with increasing lubricant thickness. This assertion is considered in Fig. 10, which presents the number of corrosion spots on a disk as a function of Zdol 4000 thickness. The results clearly indicate that lubricant thickness can contribute to corrosion protection. The number of spot counts decreases with increasing lubricant thickness upto $\sim 30 \text{ \AA}$. Interestingly, there is an increase in spot counts beyond $\sim 33 \text{ \AA}$ that is not related to corrosion. This is discussed in the following section.

2.6. Lubricant de-wetting and thickness effects

The polyperfluoroether lubricant is uniformly coated onto the disk surface. However, depending upon its molecular weight and thickness, in addition to substrate composition, and external parameters such as environment, the lubricant film may de-wet. In de-wetting, a liquid film lowers its free energy by becoming thicker in some areas, and thinner in other areas. In the computer disk industry, tribological reliability is achieved by having a continuous and uniform coverage of the carbon surface by the topically applied lubricant. Consequently, a subsequent

de-wetting of the polyperfluoroether film could impact the uniformity of surface coverage, possibly exposing potential corrosion sites; and/or facilitating lubricant pick-up by the read/write head, possibly resulting in non-uniformity of head-disk flying characteristics. We have, therefore, investigated the de-wetting of Zdol 4000 from the CN_x surface.

The droplet counts as a function of Zdol 4000 thickness on CN_x is presented in Fig. 11. The droplets represent agglomerated Zdol 4000. The de-wetting transition is clearly identified by the step increase in the observed droplet count at 32 \AA of Zdol 4000. Below 32 \AA , no de-wetting on CN_x is observed while above 32 \AA , all thicknesses show de-wetting.

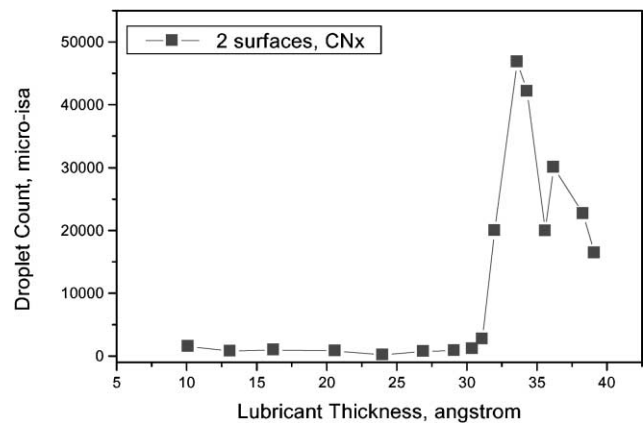


Fig. 11. Droplet counts vs. Zdol 4000 thickness on CN_x (glass substrate). The droplets are measured and counted with the optical surface analyzer (OSA) software.

Thus, the increase in counts observed previously in Fig. 10 at Zdol 4000 thicknesses $>32 \text{ \AA}$ is due to lubricant de-wetting. The de-wetting transition thickness occurs when the first monolayer thickness is exceeded. Performing a similar set of Zdol titration studies as discussed previously in Table 1, the titrated thickness for Zdol 4000 on the CN_x (glass substrates) used in these studies was $\sim 34 \text{ \AA}$. The de-wetting transition thickness provides an upper limit for the maximum thickness of Zdol 4000 that may be employed on CN_x while maintaining coverage properties.

3. Conclusions

The following conclusions are proposed on the basis of the results discussed in this paper:

1. Particulate contamination of the head–disk interface (HDI) may have a significant negative impact on the magnetic recording using low-flying proximity recording or contact recording sliders. It was shown here that particle accumulation occurs, typically, on the slider and results in sharp jumps in slider–disk clearance and friction and may cause unexpected slider–disk vibrations with possible magnetic errors resulting.
2. Lubricant mobility is an important factor in HDI design, since even a small fraction of the mobile lubricant may have a large positive effect on durability. Using one specific example, it was shown that 5 \AA of mobile Zdol lubricant improves durability 8-fold compared to the fully bonded film.
3. Lubricant mobility is not a constant for any given system: it is a strong function of time, temperature and humidity, lubricant type, and the carbon coating composition. Changing the carbon coating alone from CH_x to CN_x helps to slow down bonding the process and to introduce a larger mobile fraction during HDI burnishing, when better tribological protection is most needed.
4. One of the results of the carbon thickness reduction is disk structure corrosion, which affects not only magnetic performance, but reduces the slider–disk clearance and affects HDI durability. One possible way to control corrosion was demonstrated: thicker lubricant was shown to provide better corrosion protection.
5. Finally, we have shown that there is an upper limit in the possible lubricant thickness for any given carbon and lubricant type. Exceeding the thickness of one monolayer causes lubricant de-wetting and droplet formation. The size of these droplets is huge compared to the slider–disk clearance and will definitely affect HDI performance. Therefore, the lubricant thickness should be kept below the one monolayer thickness.

Acknowledgements

We thank R.L. White, IBM Storage Technology Division, for providing the CN_x carbon films used in Table 1.

References

- [1] S.S. Varanasi, J.L. Lauer, F.E. Talke, G. Wang, J. Judy, Friction and wear studies of carbon overcoated thin film magnetic sliders: application of Raman microspectroscopy, *J. Tribol.* 119 (1997) 471–475.
- [2] V. Prabhakaran, S.K. Kim, F.E. Talke, Tribology of the helical scan head tape interface, *Wear* 215 (2) (1998) 91–97.
- [3] R. Rottmayer, M. Donovan, Y.-T. Hsia, *Data Storage* 3 (9) (1996).
- [4] P. Herrera-Fierro, W.R. Jones Jr., S.V. Pepper, *J. Vac. Sci. Technol. A* 11 (1993) 354.
- [5] S. Mori, W. Morales, *Wear* 132 (1989) 111.
- [6] P. Kasai, *Macromolecules* 25 (1992) 6791.
- [7] L.M. Ng, E. Lyth, M.V. Zeller, D.L. Boyd, *Langmuir* 11 (1995) 127.
- [8] P. Li, E. Lyth, D. Munro, L.M. Ng, *Tribol. Lett.* 4 (1998) 109.
- [9] J.M. Meyers, R.M. Desrosiers, L. Cornaglia, A.J. Gellman, *Tribol. Lett.* 4 (1998) 67.
- [10] R.J. Waltman, *J. Fluorine Chem.* 90 (1998) 9.
- [11] J. Pacansky, R.J. Waltman, *J. Fluorine Chem.* 83 (1997) 41.
- [12] A. Khurshudov, K. Kato, Tribological properties of carbon nitride overcoat for thin-film magnetic rigid disk, *Surf. Coat. Technol.* 86–87 (1996) 664–671.
- [13] A. Khurshudov, P. Baumgart, R.J. Waltman, In situ quantitative analysis of nanoscale lubricant migration at the slider–disk interface, *Wear* 225–229 (1999) 690–699.
- [14] R.-H. Wang, R.L. White, S.W. Meeks, B.G. Min, A. Kellock, A. Homola, D. Yoon, *IEEE Trans. Magn.* 32 (1996) 3777.
- [15] R.J. Waltman, D. Pocker, G.W. Tyndall, *Tribol. Lett.* 4 (1998) 267.
- [16] R.J. Waltman, G.W. Tyndall, J. Pacansky, R.J. Berry, *Tribol. Lett.* 7 (1999) 91.
- [17] R.J. Waltman, *Chem. Mater.*, 2000, in press.
- [18] G.W. Tyndall, R.J. Waltman, D. Pocker, *Langmuir* 14 (1998) 7527.
- [19] R.J. Waltman, G.W. Tyndall, J. Pacansky, *Langmuir* 15 (1999) 6470.